Macromolecules
ARTICLE

Macromolecules **2010**, *43*, 5863–5873 **5863**
DOI: 10.1021/ma1006649

Mechanical Rejuvenation in Poly(methyl methacrylate) Glasses? Molecular Mobility after Deformation

Hau-Nan Lee and M. D. Ediger*

Department of Chemistry, University of Wisconsin-Madison, Madison, Wisconsin 53706

Received March 30, 2010; Revised Manuscript Received May 26, 2010

ABSTRACT: Optical photobleaching experiments were used to directly measure the molecular mobility of PMMA during creep and recovery to study the interaction between mechanical deformation and physical aging. Experiments were performed both on PMMA glasses with different aging histories at $T_g - 14$ K and on PMMA melts aged to equilibrium as much as 6 K below the conventional DSC T_g. Our results show that plastic deformation increases the mobility of a polymer glass, makes the system more dynamically homogeneous, and erases the predeformation aging history. After removing the stress, the highly mobile and dynamically homogeneous system quickly relaxes to a dynamically heterogeneous system. After this initial transient, glasses produced by plastic deformation follow the same aging trajectory of the thermally quenched glasses unless the strain is very large. In contrast, deformation in the preflow regime transiently increases the molecular mobility of polymer glasses but this enhanced mobility quickly returns to the original aging trajectory after unloading the stress, indicating that preflow deformation does not change the "age" of the polymer.

I. Introduction

Polymer glasses are out of equilibrium and evolve slowly toward their supercooled liquid equilibrium state in a phenomenon known as structural recovery.[1−4] As structural recovery occurs, the physical properties of a polymer glass slowly change and thus depend on the time elapsed since the glass was formed; this process is called physical aging. For example, the specific volume, entropy, and rate of segmental dynamics of a polymer glass all decrease as the sample ages. It is well-known that the changes in physical properties caused by structural recovery can be erased by heating the glass above its glass transition temperature T_g. It has also been suggested[1] that large stresses can erase the impact of physical aging, returning the glass to a less aged or even an unaged state.

The concept of "reversal of aging" or "mechanical rejuvenation" was first introduced by Struik.[1] He observed that nonlinear creep deformation in the subyield regime apparently reduced the characteristic relaxation times for viscoelastic response of a glass. He interpreted this result as a consequence of mechanically induced reversal of physical aging (mechanical rejuvenation). The rejuvenation hypothesis states that the application of a large stress to a polymer glass has the same effect as moving the thermodynamic state back toward the unaged state.[1,5] An unaged glass cannot be generated by thermal quench since physical aging already occurs during the cooling process, thus the physical properties of an unaged glass can only be accessed experimentally by extrapolation. If complete mechanical rejuvenation occurs, all the physical properties of the rejuvenated glass, such as energy and mobility, should be independent of any predeformation aging history and they should be the same as the properties of an unaged glass.

The interpretation of the mechanically induced changes in properties of polymer glasses in terms of mechanical rejuvenation is highly controversial.[5,6] *In the subyield regime,* several detailed experimental studies[5,7,8] and recent simulation work[9] have concluded that deformation-induced changes in physical properties are not associated with a change in the underlying physical aging process. *In the postyield regime,* there have been many additional tests of physical aging and mechanical rejuvenation. Boyce and co-workers[10] concluded that plastic deformation erases the aging history of polymeric materials based on the results of constant strain rate experiments and differential scanning calorimetry (DSC) measurements. In a constant strain rate compression experiment on an annealed polystyrene (PS) glass, they observed that the flow stress reached a steady-state value independent of the initial aging history. Additionally, after significant postyield deformation, the glass did not exhibit the enthalpy overshoot in the DSC measurement that is normally shown for an aged glass. Thus, Boyce and co-workers interpreted these results in terms of mechanical rejuvenation. Govaert, Meijer, and co-workers[11−13] showed that mechanical pretreatment by either rolling or torsion in the postyield range can cause a significant decrease in yield stress for PS and polycarbonate (PC) glasses. They also studied[14] the aging kinetics of PC glasses by monitoring the time evolution of the yield stress for both pretreated and thermally quenched samples. They found that the glass generated by postyield mechanical pretreatment exhibited the same rate of physical aging as that in the glass generated by thermal quench. On the basis of these observations, they concluded that the postyield mechanical pretreatment could rejuvenate a polymer glass.

However, experiments by McKenna[5,15] do not support the occurrence of mechanical rejuvenation even in the postyield regime. In experiments on epoxy glasses, they compared the buildup of the yield stress during aging of a thermally quenched glass and a plastically deformed glass. They found that the increase in the yield stress as these two samples age do not follow the same path and that the equilibrium values of the yield stress differ significantly. Hence, they concluded that the thermally quenched and plastically deformed samples are different and that plastic deformation does not rejuvenate a glass. They suggested that plastic deformation leads to an amorphous−amorphous phase transition and thus deformation creates a new state that cannot be generated by increasing the temperature above T_g. This amorphous−amorphous phase transition argument is supported by the results of a positron-annihilation lifetime spectroscopy experiment.[16]

Several groups have used simulations to study physical aging and possible mechanical rejuvenation.[9,17−21] Lacks and co-workers[18,19] used molecular dynamics simulations and energy

*To whom correspondence should be addressed.

Published on Web 06/08/2010

landscape analysis to study the influence of shear stress on the extent of physical aging in a glass. For their systems, plastic deformation increased the energy to a level that was independent of the initial state of the glass. However, they also found that plastic deformation moved the system to positions on the energy landscape that are distinct from those occupied after infinitely fast cooling. Thus, their results indicate that stress does not literally "rejuvenate" a glass. Molecular dynamics simulations by Lyulin et al.[20] also yielded a similar conclusion. They investigated the influence of thermal and mechanical histories on the internal energy of PS and PC glasses. They found that the internal energy after an extension/recompression deformation cycle is significantly higher than that of the undeformed glasses. However, they also observed that energy partitioning in the systems produced by a deformation cycle and by a heating/cooling cycle were very different. For example, for PC after a heating/fast cooling cycle, more than 80% of energy increase was due to van der Waals interactions, while after a deformation cycle, about 40% of energy increase resulted from an increase in torsional energy of the polymer chains.

Mechanical experiments have been used to infer a large increase in the molecular mobility of polymer glasses as a result of external stress and this is often considered as evidence of mechanical rejuvenation.[1,22] In such experiments, the mobility of polymer is probed by a series of small deformations after a large deformation. The analysis of these experiments is based on the assumption that the small deformations are not coupled to the large deformation and thus can be interpreted in the linear response regime. However, there is no rigorous justification for this assumption, and other interpretations are possible.[5,23] More direct experimental methods including solid state NMR,[24] case II diffusion[25] and an optical technique[26−30] have shown significant increases in molecular mobility during deformation and these results are qualitatively consistent with simulations[29,31−37] and model predictions.[38−42] However, since the measured changes in mobility are the combined effect of deformation, aging, and possibly rejuvenation, it is unclear what portion of this enhanced mobility might be due to mechanical rejuvenation.

In a previous study,[30] we used an optical photobleaching technique to quantitatively measure the segmental mobility of PMMA glasses with different aging histories during creep deformation. We observed that prior to the onset of flow, the effects of aging and stress on mobility act as independent processes; stress causes an increase in mobility, but does not erase the effect of physical aging. However, in the flow regime, plastic deformation was observed to take the glass into a high mobility state that was independent of any predeformation aging history.

The present work extends our previous study[30] and focuses on the recovery behavior of PMMA glasses after removing the stress. Experiments are designed to disentangle the combined effects of physical aging and deformation on the measured changes in mobility. For experiments at 388.7 K (T_g − 6 K) and 390.7 K (T_g − 4 K), we annealed the PMMA samples for a very long time, until equilibrium was reached, before performing the mechanical experiments. For experiments at 380.7 K (T_g − 14 K), samples with two different aging histories were employed for the measurements. Throughout the deformation/recovery experiment, we measure both the mobility and the width of distribution of relaxation times (KWW β parameter).

We find *in the preflow regime* that although external stress significantly increases the molecular mobility of PMMA glasses, the mobility returns to the original aging trajectory after the removal of stress. Thus, consistent with our earlier work, the effects of aging and stress on mobility act as two independent processes; no interruption of the aging process occurs. In contrast, *in the flow regime*, plastic deformation induces a large mobility enhancement and the system becomes more dynamically homogeneous. After unloading the stress, the highly mobile and dynamically homogeneous system quickly relaxes to a dynamically heterogeneous state that is independent of aging history. From this time forward, glasses produced by plastic deformation and by thermal quench age at the same rate and, except for very large strains, age to the same equilibrium state. Thus, our results are consistent with mechanical rejuvenation in the postyield regime after an initial transient response during which the deformed system is distinct from any thermally quenched glass or the unaged glass.

II. Experimental Section

Sample. Lightly cross-linked poly(methyl methacrylate) (PMMA) films containing 10^{-6} M probe molecules have been employed in all the measurements in this study. PMMA films were synthesized using thermally initiated radical polymerization.[27] *N*,*N*′-Dipentyl-3,4,9,10-perylenedicarboximide (DPPC) was used as the probe molecule; the chemical structure of DPPC is shown in Figure 2. The onset value of the glass transition for the PMMA is 395 K; this was measured using a TA Instruments Q2000 DSC at a heating rate of 10 K/min. Experiments were performed on samples with typical dimensions of 2.5 mm ×30 mm x 25 μm.

Local Creep Measurement. The mechanical behavior of the PMMA samples was investigated with isothermal uniaxial tensile creep experiments. A constant engineering stress, $\sigma_e = F/A_0$, was employed to deform the sample, where F is the applied force and A_0 is the original cross-sectional area of the sample. Strain was measured locally in a small region inside the PMMA sample as described in previous studies.[27,28] In brief, four photobleached lines were created on the sample by a focused laser beam to define the region (∼200 μm × 300 μm) where the local strain measurements are made. We then used a CCD camera to monitor the distance between the two lines (L_0) perpendicular to the direction of deformation; the local strain is defined as $\varepsilon(t) = (L(t) - L_0)/L_0$. L_0 is about 200 μm and as no distortion of the photobleached lines were observed we can safely assume that the deformation is always homogeneous in this small region. As described below, we performed molecular mobility measurements inside the ∼200 μm × 300 μm region. Thus, we unambiguously determine the local strain in the region where the mobility measurements are performed.

Optical Measurement of Dye Reorientation. A photobleaching technique was also used to measure the molecular mobility of PMMA[27,28] during physical aging, deformation, and recovery. All mobility measurements were performed inside the small region defined by the four photobleached lines described in the previous section. To measure mobility, we used a confocal fluorescence microscope system to perform dye reorientation measurements.[27] In these experiments, an intense linearly polarized laser beam (532 nm) is used to create a set of unbleached probes with an anisotropic orientational distribution. In time, these unbleached probes reorient and reform an isotropic distribution. This time-dependent dye reorientation process is monitored using a circularly polarized laser beam (532 nm). We separated the polarized fluorescence of the unbleached molecules induced by the weak circularly polarized laser beam into parallel and perpendicular components. The time-dependent anisotropy decay $r(t)$ is then constructed from these two components.[27]

The time-dependent anisotropy function $r(t)$ is associated with the second order orientation autocorrelation function $CF(t)$ of the absorption dipole $\hat{\mu}$ for the DPPC probe molecule, $CF(t) = r(t)/r(0) = \langle P_2[\hat{\mu}(0)\cdot\hat{\mu}(t)]\rangle$, where P_2 is the second Legendre polynomial. The measured anisotropy decays can be fit with the KWW function: $CF(t) = e^{-(t/\tau)^{\beta}}$. We then integrate the correlation function to get the rotational correlation time τ_c. The error in log τ_c is determined by how much anisotropy decays during one mobility measurement (∼360 s). The error in log τ_c is typically ±0.1 for measurements with fast anisotropy decays (more than 50% of the decay observed). The rotational correlation times for undeformed samples and for low strain experiments with slow anisotropy decays (less than 50% of the decay observed) are obtained by fitting the measured

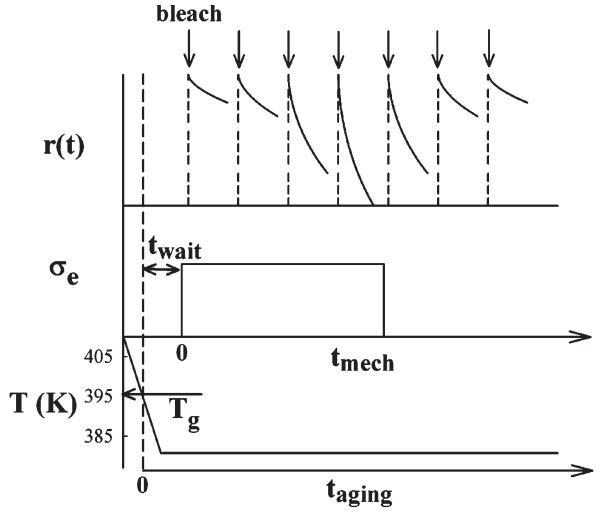

Figure 1. Schematic illustration of mobility measurement during creep and recovery. $r(t)$ is the time-dependent anisotropy decay of a low concentration probe molecule. σ_e is the engineering stress.

anisotropy decays to the KWW function with the constraint that $\beta = 0.32$. For single experiments, the error in $\log \tau_c$ is typically ± 0.2 for these slower anisotropy decays. A description of data analysis procedure and error estimation can be found elsewhere.[26,27]

Measurements of Molecular Mobility during Creep and Recovery. Figure 1 schematically shows the experimental procedure for the measurement of changes in mobility during creep and recovery. Prior to each experiment, the sample was heated to 405 K (above T_g) for at least 3 h to erase the thermal and mechanical history; the sample was then cooled to the testing temperature at 1 K/min. In this study, we refer to a sample prepared by this protocol as a thermally quenched sample. The aging time t_{aging} is defined as the time that PMMA sample spent at temperatures below the T_g measured by DSC at 10 K/min (395 K); the actual sample likely leaves equilibrium at a slightly lower temperature (~3 K), since we cool the sample at a lower cooling rate than used in the DSC experiment. We define t_{wait} as the value of t_{aging} when the stress is imposed.

Two different types of experiments are reported in this study. For experiments at 388.7 and 390.7 K, we started deformation measurements after the sample reached equilibrium ($t_{wait} \rightarrow \infty$); thus, the starting condition was a PMMA melt. For experiments at 380.7 K, equilibrium cannot be obtained in a reasonable experimental time. Instead, we performed measurements on PMMA glasses with two different waiting times (2660 s and 38660 s). For both types of experiments, a constant engineering stress σ_e was applied after t_{wait}. The mechanical experiment time t_{mech} starts at the time when the stress is applied. The local strain was recorded during both creep and recovery. For all the deformation experiments shown in this study, the samples fully recover to their original length (±0.5%) after heating above T_g for a few hours. To monitor the changes in mobility of the polymer glass during creep and recovery, we performed multiple photobleaching experiments to obtain the anisotropy decays $r(t)$ at different stages of deformation as sketched in the top panel of Figure 1.

III. Results

Temperature Dependence of Rotational Correlation Times. Figure 2 shows the rotational correlation times τ_c for DPPC in PMMA in the absence of deformation. In the melt state, the measured τ_c has the same temperature dependence as the segmental relaxation time τ_α measured by dielectric relaxation.[43] This indicates that the reorientation of DPPC is linearly correlated with the segmental dynamics of PMMA. This result is consistent with studies with other dye/polymer systems.[44−47] We assume that the reorientation of DPPC is also strongly correlated

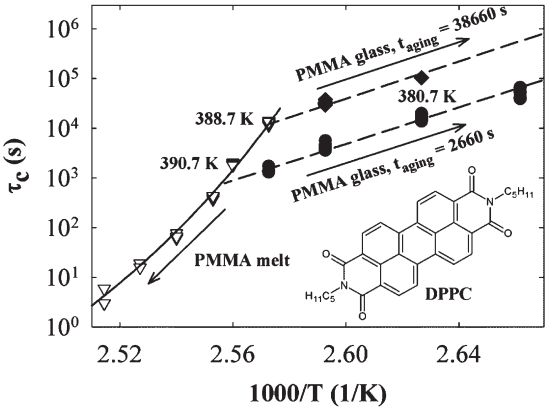

Figure 2. Rotational correlation times τ_c for DPPC in PMMA as a function of inverse temperature. The open triangles represent PMMA melts, the solid circles represent PMMA glasses measured after an aging time of 2660 s, and the solid diamonds represent PMMA glasses measured after an aging time of 38660 s. The solid curve through the melt data is the temperature dependence of the dielectric relaxation time from ref 43, shifted vertically. The two dashed straight lines through the glass data are guides to the eye. The inset shows the structure of the probe molecule used in these experiments.

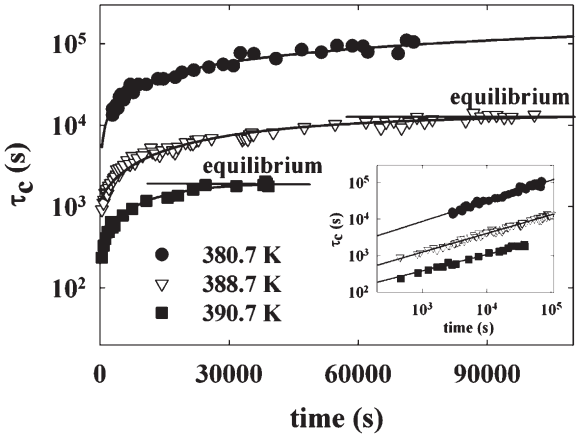

Figure 3. Evolution of the rotational correlation time τ_c for DPPC in PMMA glasses in the absence of deformation at 380.7, 388.7, and 390.7 K. The samples were cooled at 1 K/min from 405 K to the aging temperature indicated. The τ_c values lengthen due to structural recovery. For experiments at 388.7 and 390.7 K, the τ_c values appear to level off as equilibrium is approached; the long-time values of τ_c indicated in the main figure are in excellent agreement with the extrapolation of values from above T_g as shown in Figure 2. The inset is the same data plotted with a logarithmic time scale.

with the segmental dynamics of PMMA glasses during deformation. For the DPPC/PMMA system, this assumption is supported by previously reported studies.[26,28,29] In the glass state, experiments with short (2660 s) and long (38660 s) aging times are reported in Figure 2; these experiments followed the protocol of Figure 1 except that no creep experiment was performed. The dynamics of the glasses with a waiting time of 38660 s are about 10 times slower than those of the glasses with a waiting time of 2660 s.

Change in Mobility during Physical Aging. The dynamics of a polymer glass depends on the time elapsed since the glass was formed.[1−4,48] Figure 3 shows mobility measurements during physical aging at 380.7, 388.7, and 390.7 K. In each case the sample was cooled from 405 K at a rate of 1 K/min to the indicated temperature and then held isothermally. For experiments at 388.7 and 390.7 K, at first, τ_c increases with the aging time. Eventually, τ_c appears to level off at the value that we

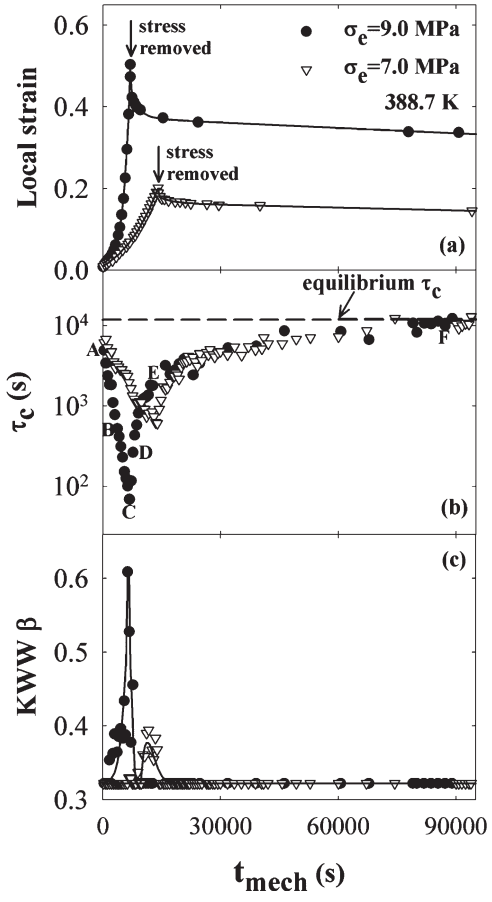

Figure 4. Changes in mobility of PMMA melts during creep and recovery at 388.7 K. (a) Local strain changes during creep with engineering stresses of 9.0 and 7.0 MPa followed by recovery. Prior to the creep experiment, these samples were annealed until reaching equilibrium. The solid lines are guides to the eye. (b) Rotational correlation times for DPPC during the creep and recovery experiments shown in the upper panel. After removing the stress, the rotational correlation times slowly recovered to the equilibrium value of τ_c for the undeformed sample. Labels A−E refer to Figure 5. (c) The KWW β parameters observed during creep and recovery.

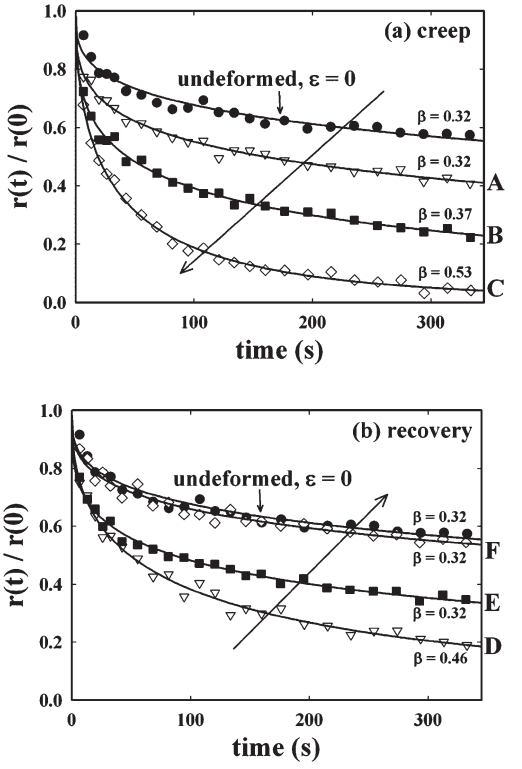

Figure 5. (a) Normalized anisotropy decays obtained during the *creep* experiment with engineering stress of 9.0 MPa as shown in Figure 4; labels A−C refer to Figure 4. As the strain rate increases, higher mobility (faster anisotropy decay) is observed. The solid lines are KWW fits to the data and the KWW β values are listed. (b) Normalized anisotropy decays obtained during the *recovery* experiment shown in Figure 4 (after creep with an engineering stress of 9.0 MPa); labels D−F refer to Figure 4. The solid lines are KWW fits to the data and the KWW β values are listed.

identify as the equilibrium value; these equilibrium values of τ_c at 388.7 and 390.7 K are shown in Figure 2. Ideally, one would wait longer (~1 week) to ensure that the samples are at equilibrium. However, given that the equilibrium values of τ_c obtained in this manner are in excellent agreement with extrapolation of τ_c values from above T_g as shown in Figure 2, we assume that aging times of 40000 s at 390.7 K and 100000 s at 388.7 K are adequate to reach equilibrium. All the deformation experiments presented in this paper at these two temperatures started after the samples reached equilibrium. For experiments at 380.7 K, equilibrium cannot be obtained in a reasonable experimental time.

The inset in Figure 3 shows a log−log plot of τ_c versus aging time. The τ_c values follow a power law behavior in the aging time. The slopes are 0.44, 0.51, and 0.56 for curves at 390.7, 388.7, and 380.7 K, respectively. This power law behavior and the decrease in slope as the temperature increases are consistent with the results of Struik's aging experiments[1] and recent simulation work.[49]

Creep and Recovery Initiated in Equilibrium PMMA Melts at 388.7 K. Figure 4 shows the changes in mobility observed during creep and recovery at 388.7 K (T_g − 6 K). In these experiments, engineering stresses of 9 and 7 MPa were applied after the sample reached the equilibrium ($t_{wait} \rightarrow \infty$); thus, the starting condition was a PMMA melt. Panel a shows the changes in strain during creep and recovery. For both experiments, the strain rate increased with time from the smallest values of t_{mech}, indicating that the sample began to flow immediately upon the application of the stress. After the stress was reduced to ~0.3 MPa, the strain slowly and partially recovered in both experiments.

During each creep and recovery experiment, we performed about 50 dye-reorientation measurements to monitor changes in the segmental mobility of the polymer at different stages of deformation. In Figure 5, we show some of the anisotropy decays measured during creep and recovery for the experiment with an engineering stress of 9 MPa. During creep, as the strain rate increased, we observed faster $r(t)$ decays, indicating higher mobility (curve A to C). During recovery, we observed slower $r(t)$ decays (curve D to F) as time progressed. These changes result solely from deformation as the sample temperature is constant throughout these experiments. As described in the Experimental Section, we fit the $r(t)$ decays to the KWW equation to determine the rotational correlation times τ_c and the KWW β exponent. Some of the fitted values of the KWW β are listed in Figure 5. The KWW β increased during creep as mobility increased and decreased during recovery as mobility decreased.

Figure 4b shows the changes in rotational correlation time τ_c during creep and recovery at 388.7 K. For the creep experiment with an engineering stress of 9 MPa, the mobility increased by a factor of 2 immediately after applying the stress, and then continually increased until the removal of the stress. After removing the stress, the mobility slowly decreased toward the mobility of the undeformed equilibrium PMMA. We

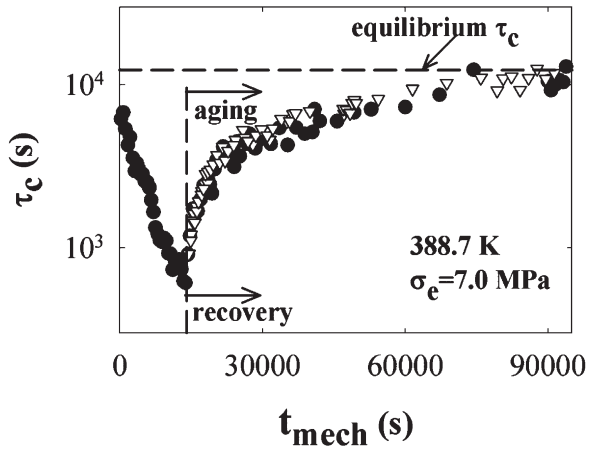

Figure 6. Comparison of molecular mobility during recovery and physical aging at 388.7 K. The solid circles are the rotational correlation times for DPPC during creep (σ_e = 7.0 MPa) and recovery. The open triangles are the time evolution of the rotational correlation times during physical aging (σ_e = 0) at 388.7 K, horizontally shifted to the time of the unloading stress.

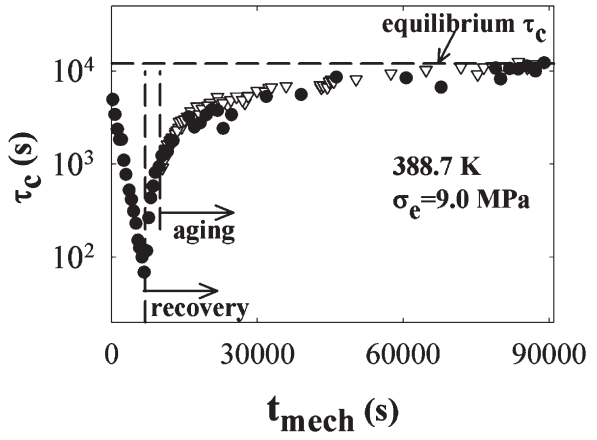

Figure 7. Comparison of molecular mobility during physical aging with mobility observed during recovery after creep (both at 388.7 K). The solid circles are the rotational correlation times for DPPC during creep (σ_e = 9.0 MPa) and recovery. The open triangles show the time evolution of the rotational correlation times during physical aging (σ_e = 0) at 388.7 K, horizontally shifted to match the recovery data.

emphasize that the mobility of the deformed PMMA fully recovered to the value of the undeformed equilibrium PMMA, even though the residual strain is still high. The creep experiment at 7 MPa has the same qualitative features as the creep experiment at 9 MPa. Figure 4c shows the changes in the KWW β parameter during these two mechanical experiments. In each case, the β parameter increases substantially when the mobility is high.

To understand how the dynamics of deformed glasses evolve during recovery, in Figures 6 and 7 we compare the mobility of glasses after deformation to that of the thermally quenched glass during physical aging. Figure 6 shows a comparison between the recovery data after the σ_e = 7.0 MPa creep (Figure 4) and the aging data (Figure 3), with both experiments occurring at 388.7 K. The physical aging data is horizontally shifted to the time of unloading stress (t_{mech} = 14045 s). Excellent agreement is observed between the recovery data and the shifted physical aging data. However, the same time shift method does not work for the recovery results after the σ_e = 9.0 MPa creep. In Figure 7,

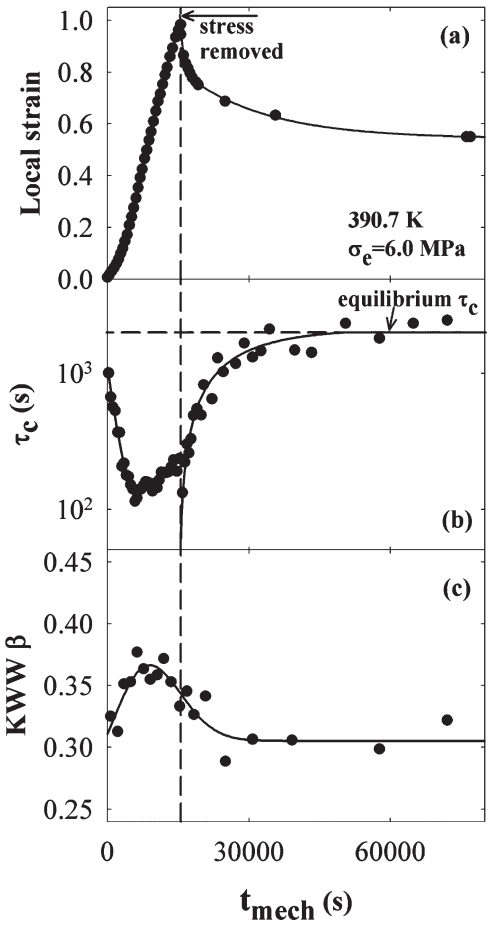

Figure 8. Mobility measurements during creep and recovery on a PMMA melt at 390.7 K. The sample was annealed until reaching equilibrium before applying an engineering stress of 6.0 MPa. Panels a−c show the time evolution of the local strain, the rotational correlation time, and the KWW β parameter, respectively. The KWW β data were smoothed using a three-point block average. The solid lines are guides to the eye.

instead of shifting the aging data to the time of the unloading of the stress (t_{mech} = 6940 s), an additional time shift of 3000 s is needed in order to match the two data sets. In both recovery experiments, the mobility of the glass clearly follows the shifted aging trajectory of the undeformed thermally quenched glass. This suggests that plastic deformation erases the previous aging history and, after removing the stress, the deformed glass ages in a manner similar to that of a thermally quenched sample. However, as shown in Figure 4c, measurements of the β parameter during first stage of recovery are elevated above the value of 0.32 observed during physical aging. This point is discussed further below.

In a creep experiment, the time under load determines the initial strain, mobility and the KWW β parameter during recovery. As a result, the amount of additional time shift required to match the recovery and aging data should depend on the time of the sample under load. A longer creep experiment at 7 MPa would be expected to yield a sample with a higher mobility and a larger β parameter, so that an additional time shift might be needed in order to match the recovery and the aging data. Similarly, a shorter experiment at 9 MPa would give a lower mobility and a smaller β parameter, and the additional time shift might not be needed in order to match the recovery and the aging data. A further discussion of the additional time shift is provided below.

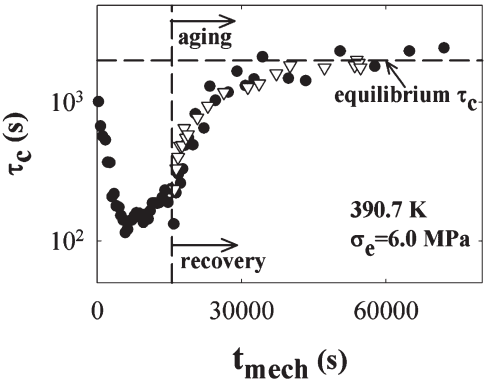

Figure 9. Comparison of molecular mobility during physical aging and during recovery following creep (both at 390.7 K). The solid circles are the rotational correlation times for DPPC during creep (σ_e = 6.0 MPa) and recovery. The open triangles are the time evolution of the rotational correlation times during physical aging (σ_e = 0) at 390.7 K, horizontally shifted to the time when the stress was unloaded.

Creep and Recovery Initiated in Equilibrium PMMA Melts at 390.7 K. Figure 8 shows the evolution of the strain and the rotational correlation time for PMMA during creep and recovery at 390.7 K (T_g − 4 K). In this experiment, an engineering stress of 6.0 MPa was applied to the sample after it aged to equilibrium. Panel a shows that the local strain rate continuously increased after applying the stress, indicating that the sample began flow essentially immediately. At ∼9000 s, the strain rate reached a maximum and then decreased very slowly; we define the onset of strain-hardening as this maximum of the local strain rate. After lowering the stress to ∼0.3 MPa, the strain slowly and partially recovered. One interesting observation is that the deformation was homogeneous for the entire experiment and the formation of a neck was not observed; for experiments at lower temperatures (Figure 4, Figure 10 and refs 26−30), necking always occurs when the strain is larger than ∼0.15.

Figure 8b shows the measured DPPC mobility during creep and recovery. Although this experiment began with an equilibrium polymer melt, the qualitative features are identical to experiments done on polymer glasses.[26,28−30] A factor of 2 mobility enhancement was observed immediately after applying the stress. As strain rate increased, the mobility continually increased until the sample entered the strain-hardening regime ($\varepsilon \approx 0.6$). At this time, dynamics are accelerated more than 20-fold relative to the undeformed polymer. In the strain-hardening regime, the mobility decreased as the strain rate decreased. After removing the stress, the mobility of the deformed PMMA first increased[26,28,29] and then slowly recovered to the mobility of the undeformed equilibrium PMMA melt.

Figure 8 (c) shows the KWW β parameter at different stages of the deformation. We smoothed the data by doing a 3-point block average. The KWW β parameter slowly increased as mobility and strain rate increased. In the strain-hardening regime, the KWW β decreased as mobility and strain rate decreased. During recovery, the KWW β parameter decreased as the mobility decreased and then stayed essentially constant at a value of 0.32. Consistent with observations from our previous studies,[26,28−30] the highest mobility enhancement always comes with the largest strain rate and KWW β value.

Figure 9 shows a comparison between the mobility of the glass during recovery (Figure 8) and the mobility of the thermally quenched glass during physical aging (Figure 3); both experiments are at 390.7 K. The qualitative features of Figure 9 are identical to those displayed in Figure 6. We horizontally shift the physical aging data to the time of unloading stress (t_{mech} = 15535 s). As in Figure 6, the mobility data during recovery clearly follows the shifted aging trajectory of the undeformed thermally quenched glass.

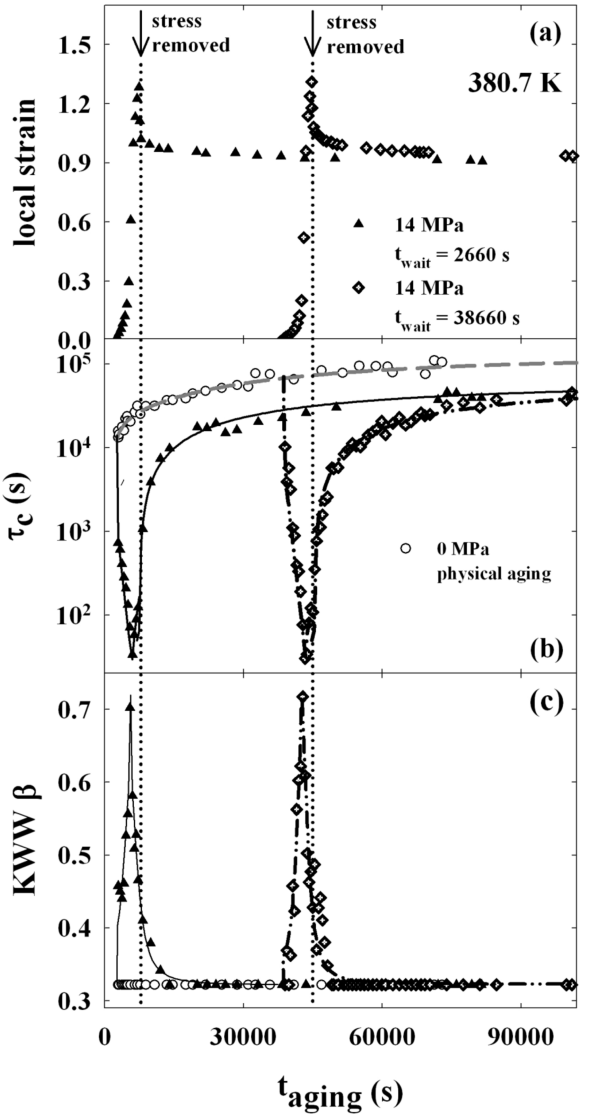

Figure 10. Changes in mobility of PMMA glasses during creep and recovery at 380.7 K. The applied engineering stress is 14.0 MPa. Experiments with short (2660 s) and long (38600 s) waiting times are presented. The data are plotted as a function of aging time t_{aging}. The lines are guides to the eye. (a) Changes in local strain during creep and recovery. (b) Rotational correlation times τ_c for DPPC during creep and recovery. The open circles are the time evolution of τ_c for DPPC in PMMA in the absence of deformation. (c) Changes in KWW β during creep and recovery. The open circles are the KWW β values during physical aging (constant at 0.32).

Creep and Recovery Initiated in PMMA Glasses: Deformation in the Flow Regime after Different Waiting Times. Creep and recovery experiments similar to those shown in the previous section were also performed on PMMA glasses at 380.7 K (T_g − 14 K). The creep experiments were initiated after short (2660 s) and long (38660 s) waiting times. The undeformed mobilities of polymer glasses with these two waiting times are shown in Figure 2.

Figure 10a shows creep experiments with an engineering stress of 14.0 MPa followed by recovery. The results are plotted as a function of aging time t_{aging}. For the creep experiment with a waiting time of 2660 s, the strain rate continuously

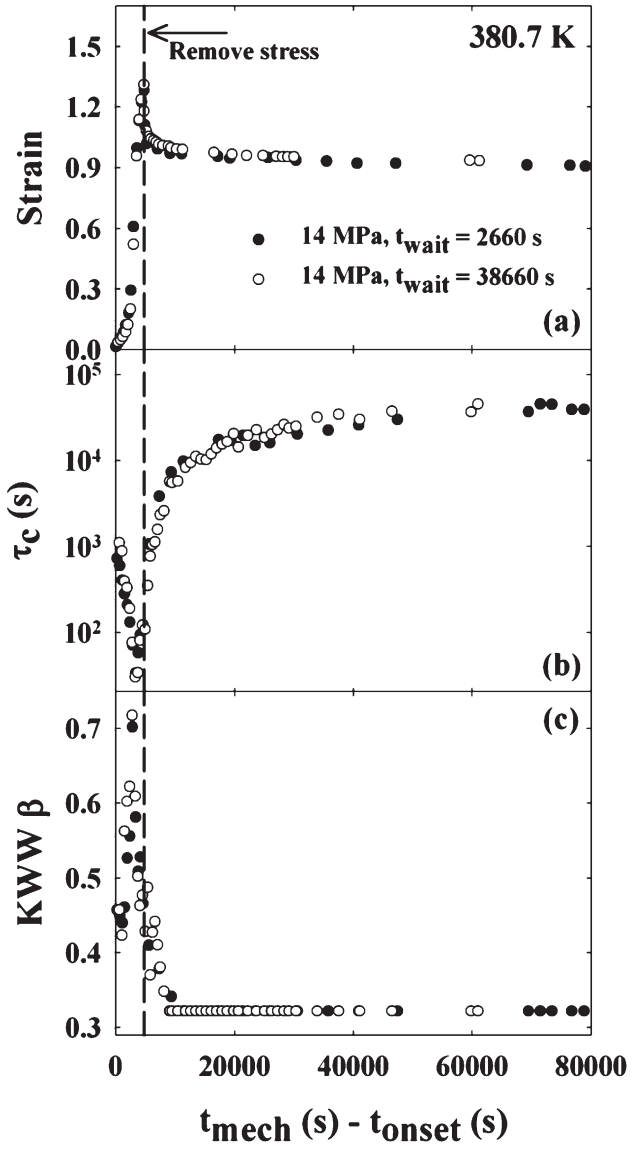

Figure 11. Changes in mobility of PMMA glasses during creep and recovery at 380.7 K. This is the same data presented in Figure 10, but here the data are plotted as a function of $t_{mech} - t_{onset}$, where t_{onset} is the time of flow onset. Panels a–c show the changes in local strain, rotational correlation times, and KWW β values during creep and recovery, respectively. After flow onset, all three observables are independent of the predeformation aging histories.

increased indicating flow from the earliest times. After ~3000 s, the strain rate started to decrease indicating that strain hardening was occurring. For the creep experiment with a waiting time of 38660 s, there was an additional preflow regime (~2000 s) in which the strain rate slightly decreased before increasing. We define flow onset by this minimum strain rate. In order to do a comparison of recovery behavior between experiments with different waiting times, we controlled the maximum strain (~1.3) before removing the stress.

The changes in mobility during creep and recovery are shown in Figure 10b. The changes in mobility during physical aging at this temperature are also shown (open circles). For the experiment with a waiting time of 2660 s, a factor of 20 mobility enhancement relative to the undeformed glass was observed immediately after the imposition of the stress. Similar to the deformation experiments on polymer melts at higher temperatures (Figures 4 and 8), the mobility continually increased as the sample flowed and then decreased after the onset of strain hardening. The experiment with a waiting time of 38860 s had lower initial mobility enhancement relative to the undeformed glass (a factor of 7). After removing the stress, the mobility slowly recovered in both experiments but did not return to the original aging trajectory.

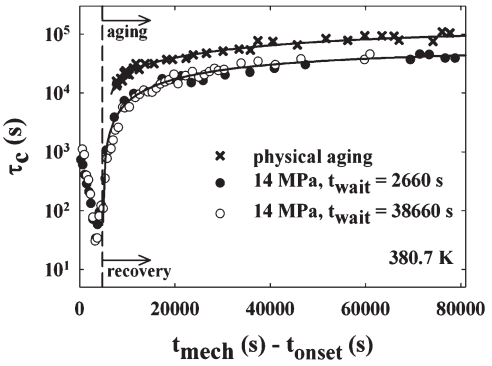

Figure 12. Comparison of molecular mobility during recovery and physical aging at 380.7 K. The circles are the rotational correlation times for DPPC during creep (σ_e = 14.0 MPa) and recovery at 380.7 K. The "×" points are the time evolution of the rotational correlation time during physical aging (σ_e = 0) at 380.7 K, horizontally shifted to the time of unloading stress. The solid lines are guides to the eye.

Figure 10c shows the changes in KWW β parameter. For both experiments, the KWW β parameter increased as the sample flowed and decreased after the onset of strain hardening. During recovery, the KWW β parameter decreased and then stayed constant. (As described in the experimental section, the β parameter is fixed to 0.32 if we observe less than 50% of anisotropy decay.) Consistent with the observations in Figure 8 and previous studies,[26,28−30] the highest KWW β value always comes with the largest mobility enhancement and strain rate.

As shown in Figure 11, we can superpose the two data sets from Figure 10 by replotting the data as a function of $t_{mech} - t_{onset,}$ where t_{onset} is the time of flow onset. After flow onset, the experiments with short and long waiting times show very similar changes in strain, mobility and the KWW β parameter during creep and recovery. This superposition works well for all three observables even though the experiment with a longer waiting time (38660 s) exhibited an additional preflow regime with decreasing strain rate and lower molecular mobility.

In Figure 12, we compare the mobility of PMMA glasses at 380.7 K during recovery to the mobility of undeformed PMMA glasses during physical aging. The physical aging data is horizontally shifted to the time of stress unloading. Unlike the comparisons shown in Figures 6, 7, and 9, horizontal time shifts cannot make the recovery curves and the aging curve superpose. We speculate that this is due to differences in the residual strain after the recovery. In this experiment, after 20 h of recovery, the strain was still very high (~0.9), while in the high temperature experiments the residual strain was smaller.

Creep and Recovery Initiated in PMMA Glasses: Deformation in the Preflow Regime after Different Waiting Times. For comparison, we also performed creep measurements on PMMA glasses with a lower stress level as shown in Figure 13. For experiments with both short (2660 s) and long (38660 s) waiting times, an engineering stress of 7 MPa was applied to the PMMA glasses for an hour and then removed. The resulting changes in local strain during creep and recovery were recorded as shown in panel a. In both experiments, the strain rate continually decreased over the entire creep

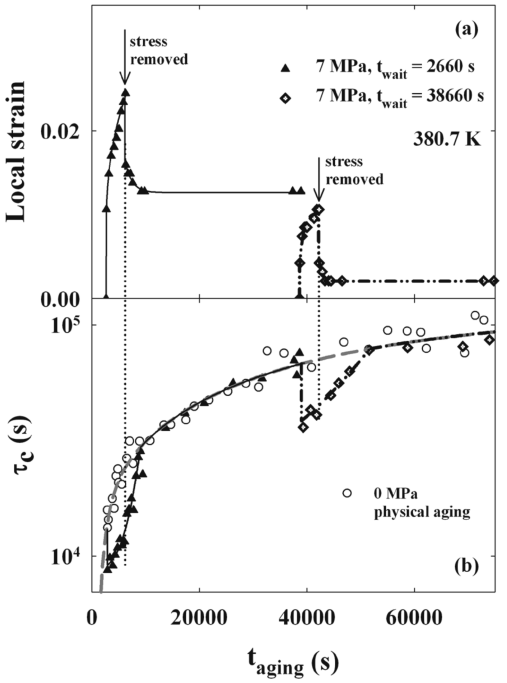

Figure 13. Changes in mobility of PMMA glasses during creep and recovery at 380.7 K with a comparison to physical aging data. Creep experiments after short (2660 s) and long (38600 s) waiting times are presented; the data are plotted as a function of aging time t_{aging}. (a) Changes in local strain during creep and recovery. The applied engineering stress is 7.0 MPa. (b) Rotational correlation times for DPPC during creep and recovery. Also shown as open circles are the time evolution of the rotational correlation time for DPPC in PMMA in the absence of deformation. The lines are guides to the eye.

experiment, indicating that the deformation stayed in the preflow regime. Small mobility enhancements (about factor of 2) were observed immediately after applying the stress in both experiments. Consistent with our observation in a previous study,[30] the mobility then slowly decreased due to physical aging. After removing the stress, the mobility returned to the original aging trajectory in both experiments. For the experiments shown in Figure 13 (and other experiments in the preflow regime), the KWW β parameter remained constant within our error limits.[26]

IV. Discussion

In this section, we first discuss our results in light of the rejuvenation hypothesis and compare to other experimental and simulation work. We then propose an interpretation of our observations using the concept of the potential energy landscape.

No Rejuvenation in the Preflow Regime. Two observations in our experiments argue that rejuvenation does not occur in the preflow regime. First, the experiments on PMMA glasses in Figure 13 show mobility enhancements during creep but in both experiments the mobility quickly returns to the original aging trajectory after removing the stress. From this, we infer that deformation in the preflow regime does not change the "age" of the sample. This observation is consistent with volume recovery measurements by McKenna and coworkers.[5,8] They measured the volume changes for an epoxy glass loaded into the nonlinear regime with torsion; after a short period of time, the torsional strain was reset to zero. They compared these results with the volume changes for an undeformed aging glass. Although changes in the volume were observed whenever the strain was adjusted, the volume at zero strain quickly returned to the value of the undeformed aging sample, indicating that nonlinear deformation does not necessarily rejuvenate a glass. Simulation work by Warren and Rottler[9] also shows a similar result. They simulated nonlinear creep in the preflow regime on a model glass system and found that the energy of the glass after deformation rose to a value similar to that of a freshly quenched glass. However, the energy gradually returned to the aging trajectory of an undeformed glass, suggesting that the underlying aging process was not modified by deformation.

A second observation from our experiments indicates that nonlinear deformation does not necessarily result in rejuvenation. In a previous study,[30] the mobility was measured during a long creep experiment at 380.7 K with an applied stress of 7 MPa. During creep the mobility slowly decreased due to physical aging and the rate of mobility decrease during creep was the same as in the absence of deformation even though mobility was about 2 times higher during creep. This observation (and others presented in ref 30) suggests that the effects of aging and stress on mobility act as independent processes prior to the flow onset. In this regime, stress does not erase the influence of aging.

As shown in several previous experiments[26,28−30] and simulations,[29,34] the changes in the properties of polymer glasses under low stress creep deformations are reasonably consistent with the Eyring model.[38] We suggest that instead of interpreting the results in the preflow regime in terms of mechanical rejuvenation, the increase in mobility in polymer glasses under preflow deformations should be attributed to an independent, transient effect due to deformation.

The experiments shown in Figure 13 allow us to test a model for physical aging proposed by Struik.[50] He proposed the following equation:

$$\frac{dv_f}{dt} = -\frac{v_f - v_\infty}{\tau[v_f, T]} + v'_{fd} \quad (1)$$

Here v_f is the free volume, v_∞ is the free volume at equilibrium, τ is the segmental relaxation time as a function of free volume and temperature, and v'_{fd} is the rate of free volume production during a mechanical deformation. In this discussion of Struik, "free volume" is synonymous with segmental mobility and can be considered to be proportional to the negative of log τ. Under these conditions, eq 1 can be rewritten as follows:

$$\frac{d(\log \tau)}{dt} = -\frac{\log \tau - \log \tau_\infty}{\tau} + \text{mobility source terms} \quad (2)$$

The meaning of eq 2 is as follows: Except during active deformation, the instantaneous segmental mobility controls the rate at which mobility will be lost over time. The data in Figure 13 is absolutely inconsistent with any equation of this type. If this equation described the data, log τ after the cessation of creep could never rejoin the original aging trajectory. Instead log τ would have to recover more slowly such that the data during recovery would look like the original aging trajectory displaced to longer times. Because our experiments are the first to directly and quantitatively measure segmental mobility during deformation, this is the first time that eq 2 could be directly tested. In contrast to eq 2, in the preflow regime the changes in mobility due to physical aging and those due to deformation are independent.

Plastic Deformation Eliminates the Influence of Prior Aging. In our experiments, aging time has no impact on the segmental mobility or mechanical properties of the polymer glass after flow onset. This is most clearly seen in Figure 11. As deformation continued into the flow regime, samples with different

aging histories exhibited equivalent mobility and strain behaviors. This observation indicates that not only the mobility during flow, but also the mobility during the subsequent recovery is independent of aging history prior to the loading of stress. Similar results were obtained in experiments with a lower stress (11.5 MPa)[30] and at higher temperature (data not shown).

Our observations are consistent with the interpretation of constant strain rate experiments by Boyce and co-workers[10] and molecular dynamics simulations by Lacks and co-workers[18,19] as described in the Introduction. This result is also broadly consistent with the mechanical pretreatment experiments by Govaert and co-workers.[11−13]

Plastically Deformed Glasses Are Not Initially the Same as Any Thermally Quenched Glass. A strict interpretation of the rejuvenation view would require that all of the (time-dependent) properties of a plastically deformed glass match those of some thermally quenched glass or the unaged glass. Our data are not consistent with this. In almost every experiment that we have performed on plastically deformed samples, the KWW β parameter in the early stages of recovery is significantly larger than the value observed for thermally quenched glasses. For these PMMA glasses, a KWW β parameter near 0.32 is found for thermally quenched samples at all aging times. By extrapolation, we expect an unaged glass to also show a KWW β value of 0.32. In contrast, Figures 4, 5, 8, and 10 all show larger values of β (up to 0.46) in the early stages of recovery. In our earlier work, values β up to 0.5 were observed in the early stages of recovery after plastic deformation.[26,28,29] These results are consistent with the simulations by Lacks and co-workers[18,19] and Lyulin and co-workers.[20] In those simulations, the state of a plastically deformed glass *immediately after deformation* was compared to quenched glasses, and clear differences were found.

Plastically Deformed Glasses Become Similar to Thermally Quenched Glasses after an Initial Transient Response. Our results at 388.7 and 390.7 K are consistent with the view that, after an initial transient associated with strain recovery, plastically deformed glasses become identical to thermally quenched glasses, since mobility, KWW β, and the time evolution of these two parameters are almost the same in these two glasses. Figures 6, 7, and 9 illustrate this for samples that were plastically deformed from equilibrium. Each of these figures show that the mobility as a function of time for the deformed sample during recovery matches the aging behavior of a thermally quenched sample (a less aged glass). At short times, as discussed above, the KWW β parameter for the recovering sample is higher than for the aging sample, but this difference is lost with time. For example, Figure 4c shows that the β parameter returns to the value of the undeformed sample in the first ~3000 s during recovery. After this, the aging behavior of the mobility for the deformed and undeformed samples is essentially identical for more than 60000 s. It is likely that the time scale required for the β parameter to return to its undeformed value is controlled by the time scale of strain recovery for these creep experiments as can be observed in Figures 4, 8, and 10. This would be consistent with the correlation that we reported earlier between strain rate and the β parameter.[26]

These results are consistent with the view that plastic deformation results in a rejuvenated sample after an initial transient. Of course, if the random error in our results were smaller or if we had additional observables, it may be that differences between the deformed and undeformed samples could be observed throughout the aging regime.

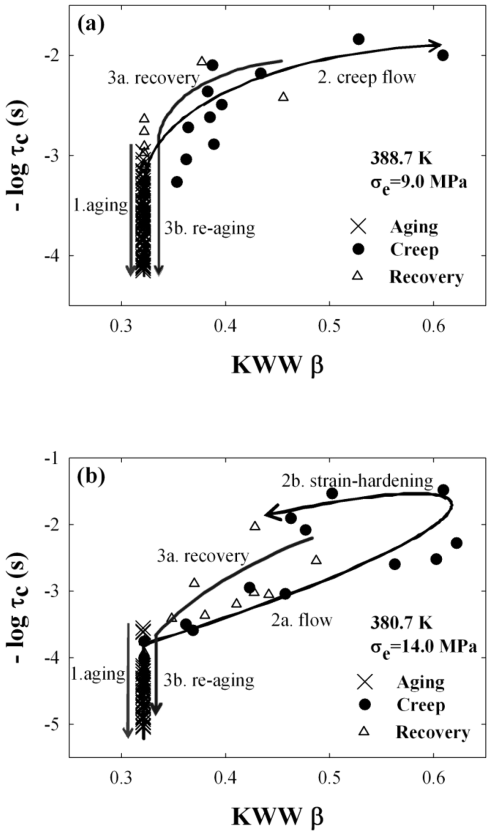

Figure 14. Interrelationship between log τ_c and KWW β during creep, recovery, and physical aging at 388.7 and 380.7 K. The cross symbols, solid circles, and open triangles represent physical aging, creep, and recovery, respectively. The lines and arrows indicate the time evolution of rotational correlation times and serve as guides to the eye. The numbers 1, 2, and 3 indicate the time sequence of the events. Panel a shows experiments at 388.7 K. The applied stress is 9 MPa. These are the data sets shown in Figure 3 and Figure 4b. Panel b shows experiments at 380.7 K. The applied stress is 14 MPa and the waiting time is 38660 s. These are the data sets shown in Figure 10.

The experiments at 380.7 K on glasses with different predeformation aging histories show identical changes in mobility during recovery (Figure 11). However in these experiments the recovery of the mobility in these samples cannot be shifted to match that of the aging undeformed glass (Figure 12). The result is unexpected in light of the discussion of the two previous paragraphs. We speculate that the reason for the mismatch is Figure 12 is the large residual strain in these samples. In this experiment, the strain was still very high (~0.9) after 20 h of recovery. We speculate that the dynamics are faster because the structure of the glass with large strain is different from that of glass with no or lower strain. Another possible explanation is that such large strains orient the polymer chains and result in a polymer glass with structure that is resistant to physical aging. This may be related to the observation of Aboulfaraj et al. that the yield stress of previously deformed epoxy samples is different than that of samples without this mechanical history, even in the limit of long waiting times.[15] From our data, we cannot exclude the possibility that at much longer times the undeformed and plastically deformed samples would age to the same equilibrium state.

Energy Landscape Description. The aging, deformation, and reaging processes can be qualitatively understood using the concept of the potential energy landscape.[51,52] Since we do not have access to microscopic information about the position of our system on the landscape, we make a

qualitative argument using our two observables. In our view, the measured mobility in our experiment can be qualitatively identified with the landscape energy; higher mobilities indicate higher energies on the landscape. This is reasonable since there is good correlation between mobility and landscape energy at equilibrium.[51] The KWW β parameter is some measure of position on the landscape at a given energy; i.e., it can be regarded as a landscape coordinate.

Figure 14 plots ($-\log \tau_c$) as a function of KWW β for mobility measurements during physical aging, creep and recovery. In panel a, we show experiments at 388.7 K with the creep experiment performed at 9 MPa. These are the same data sets shown in Figure 3 and Figure 4b. Figure 14b shows experiments at 380.7 K and utilized creep data with an applied stress is 14 MPa and a waiting time is 38660 s. These are the same data sets shown in Figure 10.

The process of physical aging lowers the molecular mobility and moves the system downward on the energy landscape (**step 1 in** Figure 14). Within a few degrees of T_g, this process can take the system to a stable mobility and landscape energy in a reasonable experimental time scale as shown in Figure 3. If we were to increase the temperature to above T_g, this would erase the effect of physical aging and move the system upward on the energy landscape (**reversal of step 1**).

Similar to increasing the temperature, plastic deformation also increases the mobility of the system, erases the previous aging history, and moves the system upward on the energy landscape. However, unlike a temperature increase, plastic deformation takes the system on a different route to a higher position on the landscape (**step 2**). Plastic deformation creates a more dynamically homogeneous system with high molecular mobility. After unloading, the dynamically homogeneous system quickly relaxes to a system that is as heterogeneous as a thermally quenched glass (**step 3a**). As a result, the system is left high on the energy landscape and in the same region of the landscape visited during physical aging. After that, the deformed glass reages, following the same aging trajectory as thermally quenched glasses (**step 3b**).

The energy landscape picture can also explain the additional 3000 s time shift that is required to superpose the data sets shown in Figure 7. Because our samples are prepared by relatively slow cooling from above T_g, the polymer glass has already aged considerably at the beginning of our experiments. A faster quench process would leave the system higher on the energy landscape. As shown in Figure 14, stress can move the system to a higher position on the energy landscape than is achieved by our preparation method. Consequently, in Figure 7, the recovering glass needed 3000 s of aging to come to a state similar to the "unaged glass" in our experiments. This observation is consistent with the experimental results of Govaert and co-workers.[14] They generated polycarbonate glasses by mechanical pretreatment, and compared the aging dynamics of these glasses to those of thermally quenched glasses by monitoring the evolution of the yield stress with time. They found that the deformed glass had a lower yield stress than the thermally quenched glass but that both glasses exhibited the same rate of physical aging.

The above discussion of the role of the potential energy landscape relies on an important assumption that we now make explicit. For a system at constant volume, a single potential energy landscape is responsible for thermodynamics and dynamics at all temperatures. During deformation, the volume of our system certainly changes – and thus the discussion of motion on a single potential energy landscape cannot be exactly correct. We assume that this volume change is not important for determining the dynamics during deformation. This view is supported by the simulations of Riggleman et al.[34] They showed substantial mobility increases during both compressive and tensile deformation even though the volume changes during these deformations were of opposite signs. The observed mobility changes for both types of deformations formed a single master curve when plotted against strain rate or inherent state energy. These observations are consistent with our assumption that volume changes are a minor contributor to the observed mobility changes during deformation.

V. Conclusions

Using an optical photobleaching method, we have directly measured the segmental mobility and the width of the associated distribution of relaxation times in PMMA during creep and recovery. Our experiments indicate that the plastic deformation not only increases the mobility in a polymer glass and forces the system to become more dynamically homogeneous, but also erases the previous aging history. After unloading the stress, the highly mobile and dynamically homogeneous system quickly relaxes to a dynamically heterogeneous system. This heterogeneous glass is very similar to a glass generated by thermal quench and can be regarded as "rejuvenated" to within the resolution afforded by our experiments. The heterogeneous glass continues to age and follows the same aging trajectory as does a thermally quenched glass. In samples with large residual strain, it appears that the deformed and undeformed glass may be aging toward different equilibrium states.

Completely different results were obtained in the preflow regime. Here the effects of deformation and aging appear act independently on the system. Active deformation accelerates mobility but during recovery the system returns to its original aging behavior, i.e., the age of the sample is not altered by deformation.

Our observations in the preflow, flow, and recovery regimes are consistent with many reports in the literature and extend them by providing direct measurements of segmental mobility during deformation and recovery. On the basis of these observations and the energy landscape picture, our description of mechanical rejuvenation for plastically deformed samples reconciles some of the apparent contradictions in the literature.[5,9,18−20] This view could be tested by future simulation work.

Acknowledgment. This work was supported by the National Science Foundation (NIRT 0506840 and DMR 0907607). We thank James Caruthers, Grigori Medvedev, Ken Schweizer, Kang Chen, Juan de Pablo, Rob Riggleman, Dan Lacks, and Alexey Lyulin for useful discussions. We thank Lian Yu and Ye Sun for performing DSC measurements.

References and Notes

(1) Struik, L. C. E., *Physical aging in amorphous polymers and other materials*; Elsevier: New York, 1978.
(2) McKenna, G. B. Glass formation and glassy behavior. In *Comprehensive Polymer Science*; Booth, C., Price, C., Eds. Pergamon: Oxford, U.K.: 1990; Vol. *2*, p 311.
(3) Hodge, I. M. *J. Non-Cryst. Solids* **1994**, *169*, 211–266.
(4) Baker, E. A.; Rittigstein, P.; Torkelson, J. M.; Roth, C. B. *J. Polym. Sci., Part B: Polym. Phys.* **2009**, *47*, 2509–2519.
(5) McKenna, G. B. *J. Phys.: Condens. Matter* **2003**, *15*, S737–S763.
(6) Struik, L. C. E. *Polymer* **1997**, *38*, 4053–4057.
(7) Lee, A.; McKenna, G. B. *Polymer* **1990**, *31*, 423–430.
(8) Santore, M. M.; Duran, R. S.; McKenna, G. B. *Polymer* **1991**, *32*, 2377–2381.
(9) Warren, M.; Rottler, J. *Phys. Rev. E* **2008**, *78*, 7.
(10) Hasan, O. A.; Boyce, M. C. *Polymer* **1993**, *34*, 5085–5092.
(11) Govaert, L. E.; Timmermans, P. H. M.; Brekelmans, W. A. M. *J. Eng. Mater. Technol.—Trans. ASME* **2000**, *122*, 177–185.

(12) Govaert, L. E.; van Melick, H. G. H.; Meijer, H. E. H. *Polymer* **2001**, *42*, 1271–1274.
(13) van Melick, H. G. H.; Govaert, L. E.; Raas, B.; Nauta, W. J.; Meijer, H. E. H. *Polymer* **2003**, *44*, 1171–1179.
(14) Klompen, E. T. J.; Engels, T. A. P.; Govaert, L. E.; Meijer, H. E. H. *Macromolecules* **2005**, *38*, 6997–7008.
(15) Aboulfaraj, M.; Gsell, C.; Mangelinck, D.; McKenna, G. B. *J. Non-Cryst. Solids* **1994**, *172*, 615–621.
(16) Cangialosi, D.; Wubbenhorst, M.; Schut, H.; van Veen, A.; Picken, S. J. *J. Chem. Phys.* **2005**, *122*, 7.
(17) Utz, M.; Debenedetti, P. G.; Stillinger, F. H. *Phys. Rev. Lett.* **2000**, *84*, 1471–1474.
(18) Lacks, D. J.; Osborne, M. J. *Phys. Rev. Lett.* **2004**, *93*, 255501.
(19) Isner, B. A.; Lacks, D. J. *Phys. Rev. Lett.* **2006**, *96*, 025506.
(20) Lyulin, A. V.; Michels, M. A. J. *Phys. Rev. Lett.* **2007**, *99*, 085504.
(21) Warren, M.; Rottler, J. *Phys. Rev. E* **2007**, *76*, 9.
(22) Martinez-Vega, J. J.; Trumel, H.; Gacougnolle, J. L. *Polymer* **2002**, *43*, 4979–4987.
(23) McKenna, G. B.; Zapas, L. J. *Polym. Eng. Sci.* **1986**, *26*, 725–729.
(24) Loo, L. S.; Cohen, R. E.; Gleason, K. K. *Science* **2000**, *288*, 116–119.
(25) Zhou, Q. Y.; Argon, A. S.; Cohen, R. E. *Polymer* **2001**, *42*, 613–621.
(26) Lee, H.-N.; Paeng, K.; Swallen, S. F.; Ediger, M. D.; Stamm, R. A.; Medvedev, G. A.; Caruthers, J. M. *J. Polym. Sci., Part B: Polym. Phys.* **2009**, *47*, 1713–1727.
(27) Lee, H.-N.; Paeng, K.; Swallen, S. F.; Ediger, M. D. *J. Chem. Phys.* **2008**, *128*, 134902.
(28) Lee, H.-N.; Paeng, K.; Swallen, S. F.; Ediger, M. D. *Science* **2009**, *323*, 231–234.
(29) Lee, H.-N.; Riggleman, R. A.; de Pablo, J. J.; Ediger, M. D. *Macromolecules* **2009**, *42*, 4328–4336.
(30) Lee, H.-N.; Ediger, M. D. *J. Chem. Phys.* in press.
(31) Lyulin, A. V.; Balabaev, N. K.; Mazo, M. A.; Michels, M. A. J. *Macromolecules* **2004**, *37*, 8785–8793.
(32) Lyulin, A. V.; Vorselaars, B.; Mazo, M. A.; Balabaev, N. K.; Michels, M. A. J. *Europhys. Lett.* **2005**, *71*, 618–624.
(33) Riggleman, R. A.; Lee, H.-N.; Ediger, M. D.; de Pablo, J. J. *Phys. Rev. Lett.* **2007**, *99*, 215501.
(34) Riggleman, R. A.; Schweizer, K. S.; de Pablo, J. J. *Macromolecules* **2008**, *41*, 4969–4977.
(35) Riggleman, R. A.; Lee, H.-N.; Ediger, M. D.; de Pablo, J. J. *Soft Matter* **2010**, *6*, 287–291.
(36) Capaldi, F. M.; Boyce, M. C.; Rutledge, G. C. *Phys. Rev. Lett.* **2002**, *89*, 175505.
(37) Capaldi, F. M.; Boyce, M. C.; Rutledge, G. C. *Polymer* **2004**, *45*, 1391–1399.
(38) Eyring, H. *J. Chem. Phys.* **1936**, *4*, 283.
(39) Argon, A. S. *Philos. Mag.* **1973**, *28*, 839–865.
(40) Robertson, R. E. *J. Chem. Phys.* **1966**, *44*, 3950.
(41) Chen, K.; Schweizer, K. S. *Europhys. Lett.* **2007**, *79*, 26006.
(42) Chen, K.; Schweizer, K. S. *J. Chem. Phys.* **2007**, *126*, 014904.
(43) Bergman, R.; Alvarez, F.; Alegria, A.; Colmenero, J. *J. Non-Cryst. Solids* **1998**, *235*, 580–583.
(44) Inoue, T.; Cicerone, M. T.; Ediger, M. D. *Macromolecules* **1995**, *28*, 3425–3433.
(45) Hwang, Y.; Ediger, M. D. *J. Polym. Sci., Part B: Polym. Phys.* **1996**, *34*, 2853–2861.
(46) Wang, C. Y.; Ediger, M. D. *Macromolecules* **1997**, *30*, 4770–4771.
(47) Dhinojwala, A.; Wong, G. K.; Torkelson, J. M. *Macromolecules* **1993**, *26*, 5943–5953.
(48) Thurau, C. T.; Ediger, M. D. *J. Chem. Phys.* **2002**, *116*, 9089–9099.
(49) Warren, M.; Rottler, J. *Phys. Rev. E* **2007**, *76*, 031802.
(50) Struik, L. C. E., In *Physical aging in amorphous polymers and other materials*; Anonymous, Ed.; Elsevier: New York, 1978; p 85.
(51) Debenedetti, P. G.; Stillinger, F. H. *Nature* **2001**, *410*, 259–267.
(52) Goldstein, M. *J. Chem. Phys.* **1969**, *51*, 3728–3739.